

Supplementary Information

A Simple Capillary-based Open Microfluidic Device for Size On-demand High-throughput Droplet/Bubble/Microcapsule Generation

Liping Mei^{a,b}, Mingliang Jin^{a,b}, Shuting Xie^{a,b}, Zhibing Yan^{a,b}, Xing Wang^{a,b}, Guofu Zhou^{a,b}, Albert van den Berg^{a,c} and Lingling Shui^{a,b*}

^a National Center for International Research on Green Optoelectronics, South China Normal University, Guangzhou 510006, China

^b Guangdong Provincial Key Laboratory of Optical Information Materials and Technology and Institute of Electronic Paper Displays, South China Academy of Advanced Optoelectronics, South China Normal University, Guangzhou 510006, China

^c BIOS/Lab-on-a-Chip group, MESA+ Institute for Nanotechnology, University of Twente, Enschede, the Netherlands

* Correspondence: shuill@m.scnu.edu.cn; Tel: +86-20-3931-4813

Forces acting on the droplet formation process in the capillary-based open microfluidic device

Since the surface of silica capillaries is hydrophilic, water (aqueous) phase works as the continuous phase and oil (organic) phase works as the dispersed phase in a typical COMD. The schematic and experimental setup is shown in **Fig. S1**.

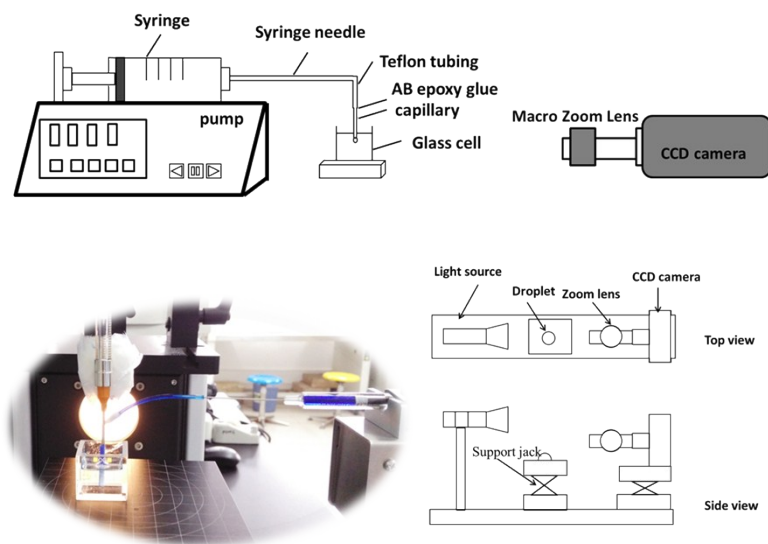


Fig. S1 Schematic diagram of the experimental set-up.

In order to making both water-in-oil (W/O) and oil-in-water (O/W) droplets, the hydrophilic capillary and quartz surfaces were treated to be hydrophobic by dipping in OTS solution¹ and spin coating a thin film of AF 1600X (Dupont, Shanghai, China).² The wettability of original quartz, OTS coated and AF 1600 coated surfaces have been evaluated by measuring the contact angles of a 2 μ L water droplet on each surface, as shown in **Fig. S2**.

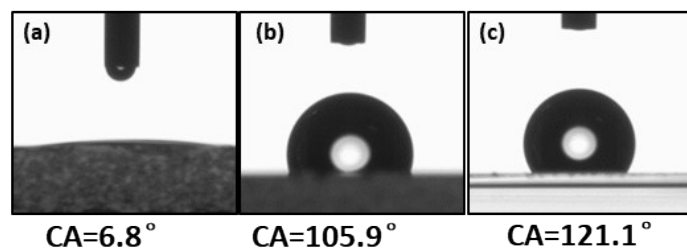


Fig. S2 Contact angle measurements of quartz surface of (a) without modification, (b) after OTS coating, and (c) after AF 1600X coating. The applied droplets are 2 μ L DI water for all measurements. CA here means contact angle.

When the capillary tip is placed close to the flat surface of the inserted quartz block or the container's bottom, the dispersed phase is infused and flow through the gap, and grows gradually to overcome the capillary force till to the edge of the gap. The droplet tip quickly expands and detaches from the capillary tip at the gap exit. **Fig. S3** shows the schematic of the droplet formation process. **Movie S1** shows the real process recorded by the digital camera of the video-based optical contact angle measuring instrument (Dataphysics OCA Pro 15, Germany). When the gap distance is large, the dispersed phase does not touch the bottom surface during a capillary dripping process. As the gap distance decreases, the dispersed phase flows out of the capillary and grows up, and then touches the bottom surface and flows along the gap formed between the capillary wall and flat bottom surface. At this stage, the gap works as a microchannel. As soon as the tip arrives at the gap edge, it quickly grows up without confinement. Therefore, a neck is formed at the capillary tip and quickly shrinking to zero. Thus, a droplet is formed and detached from the gap.

As shown in **Figs. S3a** and **S3b**, the action forces during droplet generation process is analyzed. In the experiments, $Q = 0.01-10 \mu\text{L}/\text{min}$, and the corresponding capillary I.D. = $20 \mu\text{m}$ and O.D. = $88 \mu\text{m}$. The dispersed flow velocity u_f at the capillary tip is calculated as: $u_f = Q/\pi r^2$ (r is the inner radius of capillary) which is in the range of $0.53-530 \text{ mm}/\text{s}$. The continuous water phase is assumed to be static since there is no external flow in this COMD. The viscosity of water and oil phase is about 1.0 and $3.45 \text{ mPa}\cdot\text{s}$, respectively; and their density is 0.98 and $0.73 \text{ g}/\text{mL}$ at $25 \text{ }^\circ\text{C}$, respectively. The interfacial tension between water (3 wt% SDS) and hexadecane was measured to be $\sim 5.0 \text{ mN}/\text{m}$.

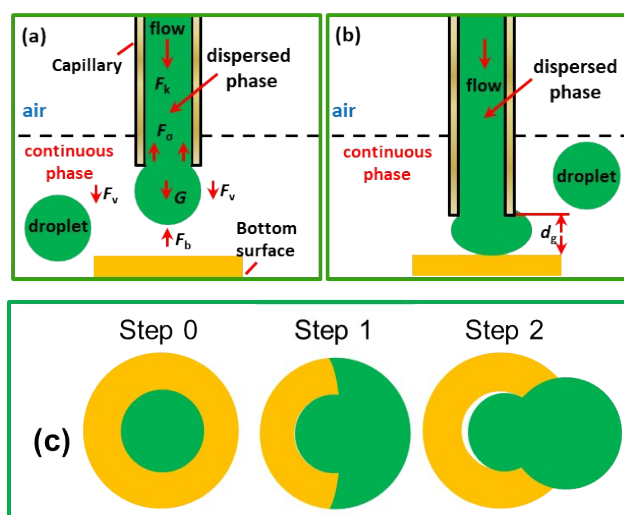


Fig. S3 (a) Forces involved during droplet formation process. (b) The inner phase tip touches the bottom, flows along the gap, and detaches from the exit. (c) Schematic of the dispersed phase flowing from the capillary tip to edge and breakup into droplet. Here, the involved forces are: F_o - water-oil interfacial tension; F_v - viscous drag force; F_k - kinetic force; G - droplet gravity; F_b - the buoyance on the droplet; d_g - the gap distance between the flat capillary tip and bottom surface.

There are five possible forces influencing the droplet generation: capillary, viscous, inertial, buoyance and gravity forces, as shown in **Figs. S3a** and **S3b**. **Table S1** shows the formula of calculating these forces. The continuous (outer) phase is assumed to be static; thus, the kinetic force is from the flow of inner phase. The interfacial tension is a constant when the material system is fixed. The viscous is related to both fluid viscosity and flow velocity. In this device, only continuous phase is flowing, all flow velocity is from the inner phase (u_f). Buoyance and gravity forces are combined and presented as their difference caused by their density difference.

From **Table S1**, we find that the interfacial tension effect is dominant whereas the inertial effect (F_k), gravity (G) and buoyant forces (F_b) could be neglected. When the capillary tip touches the bottom surface, during which the droplet is forced to deform to overcome the capillary force and detaches from the capillary tip at the edge. Touching the bottom surface is found to be the key factor in this COMD, forcing the dispersed phase to be confined in the gap. Afterwards, the dispersed phase flows through the micro-gap and then detaches from the gap forming a neck at the capillary exit. Therefore, the governing force is from F_σ in the neck, which quickly make the dispersed phase to break to generate a droplet. Without touching the surface, the viscous drag force F_v could hardly be overcome by F_σ in the regime of small velocity. After a droplet detached from the gap, the lower-than-water density of the hexadecane allowed for the settlement of the droplets to the top the continuous phase. Details of the droplet generation process in **Movie S1** validates our hypothesis that the droplet detachment occurs at the touching process. The droplet generation frequency increases and the droplet size decreases with decreasing gap distance (d_g).

Table S1 Main forces acting on the droplet formation process.

Force	Equation	Magnitude of calculated value
Water-oil interfacial force F_σ	$F_\sigma = 2\pi r\sigma$	$\sim 10^{-7}$
Viscous force F_v	$F_v = 6\pi\mu r\mu_f$	$\sim 10^{-8}$
Difference of gravity and buoyance ΔF_b	$\Delta F_b = \Delta\rho gV$	$\sim 10^{-10}$
Kinetic force F_k	$F_k = \rho Q\mu_f$	$\sim 10^{-10}$

For deeper analysis, the dimensionless numbers of Capillary number: Ca ($Ca = \mu_f u_f d / \sigma$, the ratio of viscosity to capillary effects), Reynolds number: Re ($Re = \rho u_f r / \mu$, the ratio of inertial over viscosity effects), Bond number: Bo ($Bo = \Delta\rho g r^2 / \sigma$) are employed to demonstrate the ratio of gravity to interfacial effect. **Table S2** summarizes the forces and relative dimensionless number involved in the droplet formation. Based on the given values, $Ca \sim O(10^{-2})$, $Re \sim O$

(10^{-1}) and $Bo \sim O(10^{-5})$ are obtained, suggesting that the capillary effect is dominant while gravity and inertial effect could be neglected to simplify the analysis. It is worthwhile to mention, the flow rate/velocity used for data presentation and calculation is from the inner phase flow (Q for volumetric flow rate, u_f for flow velocity) since the continuous phase is static at the beginning and very small when forced to flow by infused inner phase. Thus, the outer continuous phase flow is assumed to be zero in this work.

Table S2 Dimensionless numbers of Capillary, Reynolds and Bond numbers.

Dimensionless Number	Equation	Meaning	Magnitude of calculated value
Capillary number Ca	$Ca = \mu u_f / \sigma$	Viscosity effect/capillary effect	$\sim 10^{-2}$
Reynolds number Re	$Re = \rho u_f r / \mu$	Inertial effect/viscosity effect	$\sim 10^{-1}$
Bond number Bo	$Bo = \Delta \rho g r^2 / \sigma$	Gravity effect/capillary effect	$\sim 10^{-5}$

In this table, the parameters are set to be: ρ , the density of the pure water (1.0 g/mL), g , the acceleration of gravity (9.8 N/Kg), Q , the flow rate of the dispersed phase (1.0 $\mu\text{L}/\text{min}$), u_f , the flow velocity of the inner phase at the capillary tip, r , the inner radius of the capillary (10 μm), σ , the interfacial tension between the water and the oil phases, and μ , the viscosity of the continuous phase (1.0 mPa.s).

To describe the relationship between generated droplet size and its influence factors, the Capillary number of dispersed phase (Ca) is used here. Ca is defined as the ratio of viscous force to interfacial force, which is calculated by $Ca = \eta v / \sigma$, where η , v and σ are the viscosity, the flow velocity and interfacial tension, respectively. In this COMD, since continuous phase flow is zero, the viscosity of dispersed phase is applied and the flow velocity is calculated by dividing the dispersed phase flow rate by the inner cross-sectional area of the capillary (capillary diameter related). The experimental data of droplet diameter (D) at different flow rate for each gap distance are plotted versus Ca , as shown in **Fig. S4**. It can be clearly observed that there are two distinct regimes for the variation of droplet diameter at different Ca at a constant gap distance.

In Regime I, when $Ca < 10^{-3}$ the droplet diameter remains at a fixed value (dash line in Regime I) with deviation of about 5%, which is determined by the gap distance. The droplet diameter increases linearly with gap distance for the same capillary (Fig. 3g), being unaffected by Q and Ca . In Regime II, D changes linearly with Ca , as described by the following **Eq. S1**.

$$D = \alpha + \beta Ca, \quad (\text{S1})$$

where D is the droplet diameter, Ca is the capillary number, the coefficients of α and β can be determined for each gap distance. Physically, α is related to the filling process in which the disperse phase gradually occupy the gap, while β reflects

the deformation process in which the dispersed phase is continuously pumped into the deformed droplet during its detachment from the capillary tip into continuous phase. The values of R^2 in the inset of **Fig. S4** indicate excellent linearity between the droplet diameter and Ca in Regime II. Therefore, for a given capillary tube, it is possible to use **Eq. S1** to predict the droplet size at different Ca or Q at each gap distance.

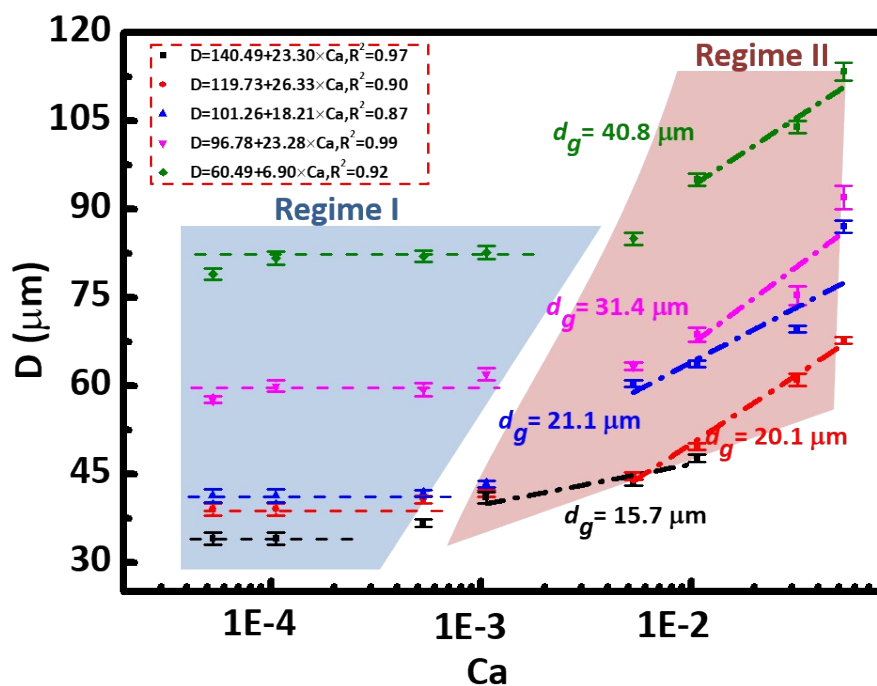


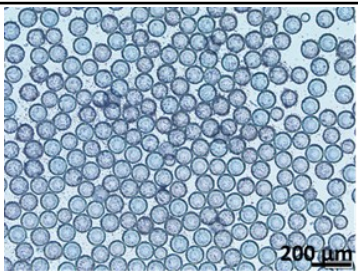
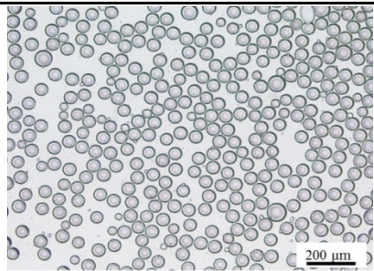


Fig. S4 Droplet diameter (D) vs. Capillary number (Ca). Generated droplet diameter is not sensitive to Ca in Regime I (highlighted in blue). The dash lines in Regime I indicate the average droplet diameters for each gap distance. The droplet diameter *increase* linearly with Ca in Regime II (highlighted in pink). The dash lines in Regime II are the linear fitting equations ($D = \alpha + \beta Ca$) for the relationship between D and Ca at each gap distance. The values of coefficients (α , β) for each gap distance are listed in the inset.

In Table S3, the details about the W/O droplets formation process and parameters are presented. Two types of oil phases (O_1 and O_2) and two corresponding water phases (W_1 and W_2) were prepared to make stable W/O droplets using a COMD.

Table S3 The detailed information about the W/O droplets.

Oil phase (O)	3 wt% Span 80 in n-Hexadecane solution (O_1)	Mixture of mineral oil and n-tetradecane at a ratio of 1:1 (v/v), containing 3 wt% ABIL EM 90 (O_2)
Water phase (W)	Methylene blue dissolved in DI water at concentration of 50 mg/L (W_1)	DI water (W_2)
Images of water droplets in the oil phase		
Interface tension σ (mN/m)	2.99	15.8
OTS modified capillary	i.d.=88 μm , o.d.=20 μm , contact angle of OTS modified glass is $\sim 100^\circ$	
Generated water droplets		
	$D = 75 \mu\text{m}$ at $d_g = 55.5 \mu\text{m}$, $Q = 0.1 \mu\text{L}/\text{min}$	$D = 48 \mu\text{m}$ at $d_g = 20.2 \mu\text{m}$, $Q = 0.1 \mu\text{L}/\text{min}$

Description of movies for droplet generation using various fluidic materials

Movie S1: Using capillary of (I.D.=20 μm , O.D.=88 μm) in this COMD device, the **O/W** (the hexadecane oil in SDS solution) droplet size changes continuously with d_g , and quickly reaches a stable size and generation frequency at a constant flow rate of 0.1 $\mu\text{L}/\text{min}$.

Movie S2: The generation process of **W/O droplets** (water droplets in HFE 7500 solution) at $d_g = 29.3 \mu\text{m}$ and $Q = 0.1 \mu\text{L} / \text{min}$ using a capillary of I.D.=20 μm and O.D.=88 μm .

Movie S3: The generation process of **air bubbles** in 2.53 wt% SDS aqueous solution at $d_g = 48.4 \mu\text{m}$ and $Q = 1.0 \mu\text{L} / \text{min}$ using a capillary of I.D.=20 μm and O.D.=88 μm .

Movie S4: The generation process of **liquid crystal (5CB) droplets** in water at $d_g = 55.5 \mu\text{m}$ and $Q=1.0 \mu\text{L} / \text{min}$ using a capillary of I.D.=100 μm and O.D.=365 μm .

Movie S5: The generation process of **ETPTA pre-polymer droplets** formed in water at $d_g = 38.3 \mu\text{m}$ and $Q= 1.0 \mu\text{L} / \text{min}$ using a capillary of I.D.=100 μm and O.D.=365 μm .

Movie S6: A movie of the O/W (the hexadecane oil in SDS solution) droplet generation process of **10 capillary arrays** at $Q=1 \mu\text{L}/\text{min}$ and $d_g \sim 15.3 \mu\text{m}$ using a capillary of I.D.=20 μm and O.D.=88 μm .

References

1. L. Shui, A. van den Berg, J. C. Eijkel, *Lab Chip*, 2009, **9**, 795-801.
2. T. He, M. Jin, J. C. T. Eijkel, G. Zhou, L. Shui, *Biomicrofluidics*, 2016, **10**, 011908.